Towards Marine Bloom Trajectory Prediction for AUV Mission Planning

Jnaneshwar Das*, Kanna Rajan†, Sergey Frolov†, Frederic Py†, John Ryan†, David A. Caron‡, Gaurav S. Sukhatme*
*Robotic Embedded Systems Laboratory, Department of Computer Science, University of Southern California
†Monterey Bay Aquarium Research Institute, Moss Landing, California
‡Dept. of Biological Sciences, University of Southern California
jnaneshd@usc.edu, {kanna.rajan,frolovs,fpy,ryjo}@mbari.org, {dcaron,gaurav}@usc.edu

***Abstract*— This paper presents an oceanographic toolchain that can be used to generate multi-vehicle robotic surveys for large-scale dynamic features in the coastal ocean. Our science application targets Harmful Algal Blooms (HABs) which have significant societal impact to coastal communities yet are poorly understood ecologically. Bloom patches can be large spatially (in kms) and unpredictable in their extent. To understand their ecology, we need to be able to bring back water samples from the 'right' places and times for lab analysis. In doing so, we target hotspots representative of intense biogeochemical activity for such sampling. Our approach uses remote sensing data to detect such hotspots using ocean color as a proxy, and advectively projects these patches spatio-temporally using surface current data from HF Radar stations. Experiments with satellite and Radar data sets are promising for large, coherent blooms. We show how these predictions can be used to select an appropriate sampling trajectory for an AUV.**

I. INTRODUCTION

Observing large scale oceanographic features has often been difficult. For example, Intermediate Nepheloid Layers (INL) are near-coastal fluid sheets of suspended particulates with large horizontal extent (in kilometers) and small vertical extent (in 1-10 meters). Harmful Algal Blooms (the focus of this paper) are likewise spread over kilometers with primary productivity driving its ecology within the top 5-10 meters. Traditional approaches using ship-based measurements for observing such dynamic and episodic phenomenon have proven to be ineffective given evolving biological state, the need to measure various properties across the spatial extent of such phenomenon, and most of all in dealing with logistical details centered on manned ships on fixed schedules.

More recently Autonomous Underwater Vehicles (AUVs) have shown to be more cost-effective, have demonstrated increased persistent presence, and with a suitable sensor payload have been able to systematically observe large scale phenomenon at requisite scales of variability of bio-geochemical processes [1], [2]. Yet, such mobile robotic assets have often been ineffective in resolving the spatio-temporal characteristics to effectively sample and observe. Additionally while satellite observations have proven to be helpful, they are constrained either by cloud cover, the lack of data beyond a meter or two of the sea surface (when process driven phenomenon can and are often within the euphotic zone upto 150m in depth) and logistical issues with the time lag between observations and processed data sets available for use. Mooring data suffers from a spatial sparseness even if in-situ measurements are accurate and available in real-time.

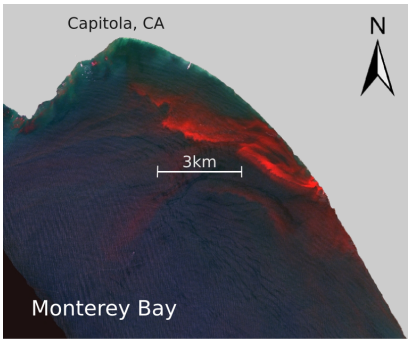

Fig. 1. NIR-G-B composite image of NE Monterey Bay on August 26, 2004, when an extremely dense red tide bloom was present.

Our goal and the subject of this paper is to make use of the data available from a range of sources including ocean models, remote sensing satellites, moorings, and on-shore instruments to make predictions of the trajectory of a patch of water. We target HABs for a number of reasons.

Phytoplankton blooms can not only drive rapid CO_2 sequestration but, also generate conditions harmful to other organisms in the case of Harmful Algal Blooms (HABs). These blooms have large spatial (> 50 km^2) and temporal extent and are visible from space as coloration of the ocean surface. Ocean physics occurring on small scales can contribute to the dense aggregation of red tide blooms [3]. The red tide image in NE Monterey Bay in Fig. 1 shows a narrow band of extremely high near-infrared reflectance (a characteristic signature and a basis for quantifying bloom intensity).

However, the drivers and mechanistic processes behind bloom initiation, evolution and collapse are not well understood in part due to the complex interactions between the members of the microbial communities and the surrounding environment. As a result, our capacity to assess the range of potential future scenarios that might result from ocean temperature changes, acidification, or nutrient shifts is highly limited. The causes and triggers for these blooms vary widely depending upon regional geography and consequent oceanography [3]. Accurately predicting the location and time of a HAB onset or demise is a difficult task, and an open problem. Finally, prediction of bloom collapse is relevant to societal needs, including early re-opening of closed fisheries due to bloom toxicity, warning of possible intensification of harmful effects in a dying bloom, and predicting the onset of anoxic events.

The direct impact of HABs is the introduction of toxins into the marine (and as a consequence human) food chain.

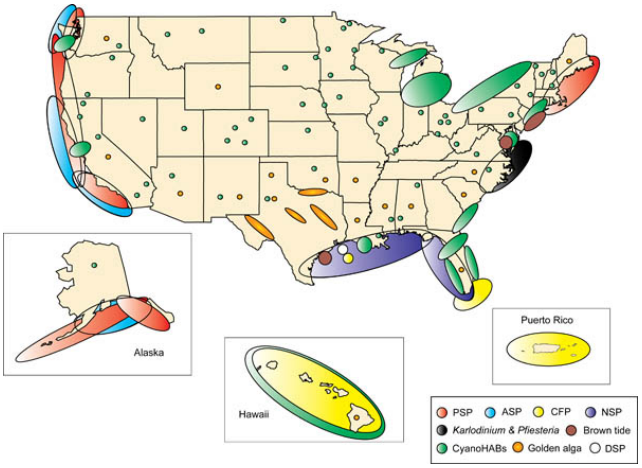

Fig. 2. U.S. coastal areas affected by various HAB toxins, syndromes and impacts (from [6])

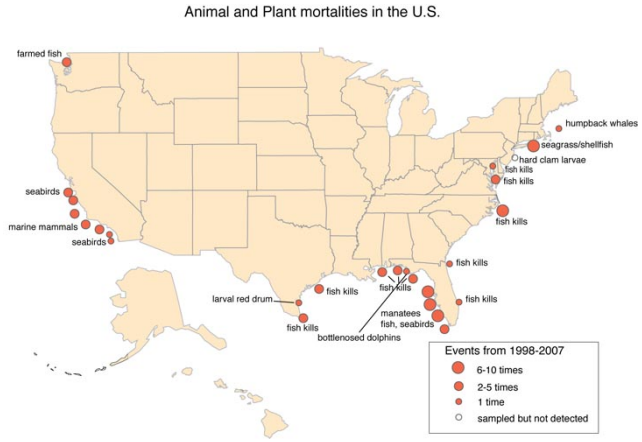

Fig. 3. Animal and Plant mortalities due to HABs (from [6])

In addition, [4] and [5] estimate that the average economic impact resulting from HABs in the US is ∼$75 million from 1987 to 2000. Fig. 3 shows plant and animal mortalities tracked from 1998 to 2007.

The causes and triggers for these blooms vary depending upon regional characteristics and the ocean current system. To understand the bloom ecology (why and when they occur, and why they decay), it is necessary to sample bloom hotspots (regions with very high biochemical activity) with high spatio-temporal resolution. To plan survey missions, scientists rely on satellite imagery, data from moorings and drifters, ocean models, and seasonal patterns in observing HABs with the goal to maximize the likelihood of sampling hotspots as well as to be able to stay with a patch of the water with such intense activity. However predicting the occurrence of a bloom is a difficult task given the complex variability in coastal waters coupled with rudimentary understanding of phytoplankton ecology [7]. Because of the non-localized nature of blooms, the size of the observation area, and the lack of understanding of the exact dynamics, ship-based and AUV missions often under-sample bloom hotspots. Factors negatively impacting mission success include the lag in obtaining processed satellite data (usually 1-2 days), and the spatial sparsity of mooring data. Additionally, plans are made in an ad-hoc, per deployment basis and cannot be generalized to be used in a continuous, repeatable manner.

In recent work [8]–[10] at USC Center for Integrated Networked Aquatic PlatformS (CINAPS) [11], gliders were used to track fresh water plumes based on ocean current predictions from the Regional Ocean Modeling System (ROMS) [12] model. [3] discusses the effect of external forcing on blooms occurring in the Monterey Bay. Our effort is complementary and leverages the above effort in addressing a piece of the larger problem: how to predict the trajectory of an algal hotspot. As robotics technologists, our ultimate aim is to design sampling surveys as a means to decide whether one or more robotic assets will be needed to sample a dynamic field. When more than one asset is available, we wish to determine where to deploy such assets given the large spatial extent of blooms. And finally we wish to motivate the design of intelligent coordination algorithms when multiple assets are deployed to ensure such configurations are robust to the harsh environmental conditions.

Our experiments target the Monterey Bay which is not only one of the most biologically diverse bodies of waters but the northeast bay frequently experiences extreme "red-tide" blooms, making it an ideal location for bloom studies. In this paper we analyze the result of advecting hotspots from blooms that occurred between October 2007 and October 2008 at the Monterey Bay, and show an example of how such predictions can be used to plan survey missions for AUVs.

The paper is organized as follows. Section II gives a brief overview of data sources, the key projection algorithms and motivations for using these approaches. In section III we analyze the results of our experiments and follow it up with sample AUV survey designs in section IV. Finally we conclude our findings and briefly articulate future work in section V.

II. System Description

The dynamics of an algal bloom can be primarily described by three factors: advection, diffusion, and bloom ecology. Advection is the component of the transport that is due to the effect of external forcing (ocean current). Diffusion results from movement of particles along concentration gradients. Lastly, since the phenomenon is biological, its growth and decay is governed by bloom ecology. To predict the dynamics of the bloom for long timeframes (*e.g.,* months) would require data for all three factors described above. However, for a strong coherent bloom already in progress, predictions can be made for for a period of upto a week based on the external forcing and diffusion. Ocean observing systems such as SCCOOS [13] and CeNCOOS [14] provide near-realtime data on various aspects of the physical sea-state such as temperature, current, salinity and sea surface height. Given access to these data, we ignore ecology and diffusion and focus on the advective effect of ocean currents on blooms.

Our system computes prediction of bloom trajectories in two steps,

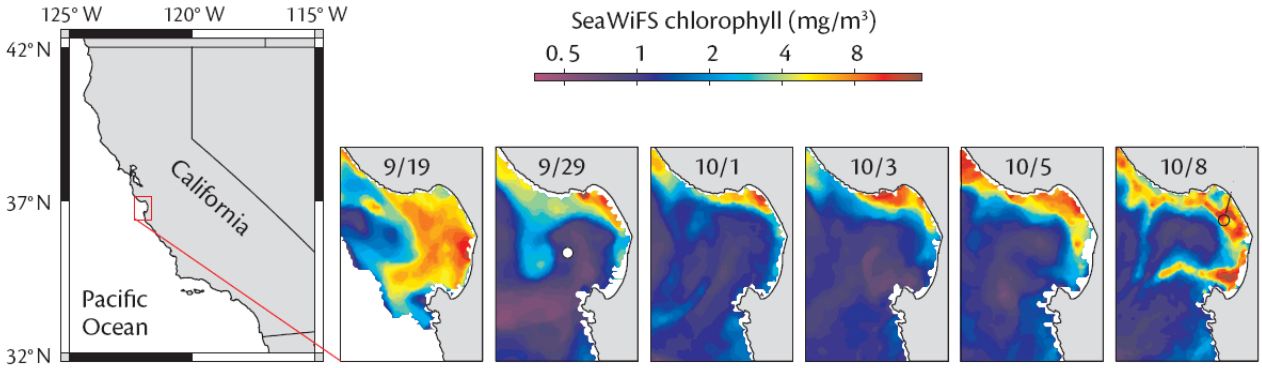

Fig. 4. SeaWiFS images showing a red-tide bloom at the Monterey Bay between September and October 2002 [3]

1) patches of bloom hotspots are detected from remote sensing data,
2) detected patches are advected using surface current data from HF Radar stations.

In this section we first discuss the data sources and then describe how we perform these two steps.

A. Data Sources

1) Remote Sensing Data: Remote sensing satellite data provides a synoptic view of the oceans, enabling bloom detection by use of proxy measurements, such as ocean color and emitted radiance due to fluorescence. One example is the MODIS (MODerate resolution Imaging Spectroradiometer) instrument on NASA's Terra and Aqua Earth-orbiting spacecraft [15]. Both Terra and Aqua view the entire Earth's surface every one to two days. One of the data products from the Terra MODIS is Fluorescence Line Height (FLH), a relative measure of the amount of radiance leaving the sea surface in the chlorophyll fluorescence emission band ($\sim$ 685 nm), at a resolution of 1 km [16], [17]. FLH is a recognized proxy for chlorophyll concentration in the upper column of water[1] [18]. Another example is the Sea-viewing Wide Field-of-view Sensor (SeaWiFS) and the chlorophyll-a data product. Fig. 4 shows a strong bloom in the Monterey Bay that occurred between September and October 2002.

MODIS data in particular, are available in Hierarchical Data Format (HDF) where the FLH data product from each MODIS image can be read into a 500 x 667 matrix.

2) High Frequency Radar Data (HF Radar): External forcing by wind and water currents is a dominating factor in bloom transport, providing reasonable estimates of the trajectory of hotspots over a period of few days using only external forcing. We used surface current data obtained from HF Radar stations maintained by CeNCOOS, which provides radial ocean surface current information in near-real time. With data from multiple stations, the velocity components of the surface current is computed. The data must be filtered, interpolated and extrapolated. In our experiments, we obtained Open-Boundary Modal Analysis (OMA) interpolated radar data for the period October 2007 - October 2008 (see Fig. 5 for an example). While the work presented can be can be used with the ROMS model surface current projections, our analysis is on archived data to validate bloom projection. Fig. 6 illustrates the data sources and the time-line of predictions.

[1]The volume of water $<$ 10 m from the surface.

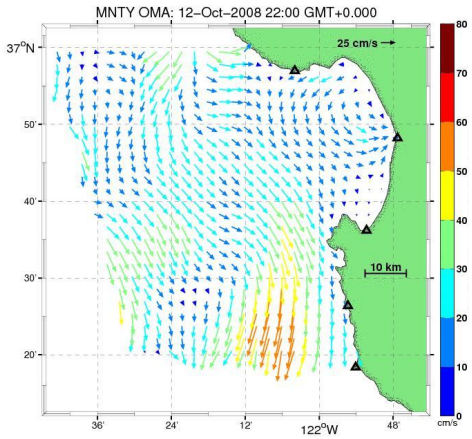

Fig. 5. Open Normal Mode Analysis (OMA) modeled hourly current vectors for the Monterey Bay [14]

B. Hotspot trajectory prediction

1) Hotspot detection: We define a bloom hotspot as the region in a MODIS image M in which the pixels have FLH values f that are greater than a specified threshold F. This is a proxy for a region of intense biological activity. The thresholded image is referred to as $I_{thresholded}$. For our purposes of asset placement, we want to track multiple hotspots. Thus, we label the k selected patches as $H = \{h_1, h_2, .., h_k\}$. Since advecting each pixel within a patch over multiple time steps is computationally expensive, we choose a sparser representation of a patch. For each $h_i \in H$, $i \in 1, ..., k$ we select representative points to be advected. These representative points may be from the convex hull, lie on the boundary, are from the interior, or are the centroid of the patch.

2) Hotspot advection: Hourly HF Radar data is available at a 2 Km resolution in a gridded format. We interpolate the HF Radar surface current estimates so that for any location $p = [x \quad y]^T$ (x, y are longitude and latitude, respectively), and time t, we have the surface current velocity $R_{p,t} = [u \quad v]^T$, where u and v are the East and North velocity components respectively. A sample is defined as $s = [p^T \quad f]^T$ where f is the FLH value at location p. Each

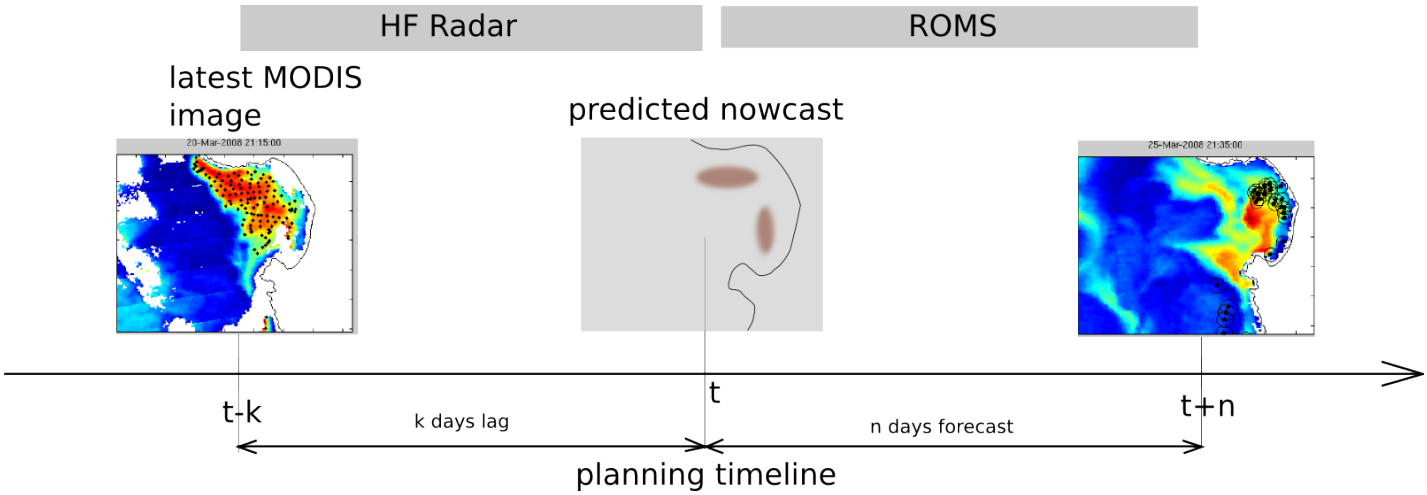

Fig. 6. Illustration of a scenario where a satellite image is obtained with a lag. HF Radar data is used to generate prediction of bloom locations. ROMS forecast of ocean current can be used to generate predictions into the future for bloom locations.

point p within a patch is projected using $R_{p,t}$ to obtain a new position of the sample point $p_{t+1} = p_t + R_{p,t+1}\Delta t$ The error covariances for the OMA interpolated velocity estimates are given as σ_u and σ_v for each data point in the grid. These are used to project the estimation error of the advected point. The new error is obtained by $\sigma_{p_{t+1}} = \sigma_{p_t} + \sigma_{R_t}\Delta t$. Algorithm 1 summarizes the process of detection and advection of bloom patches. In our current implementation, we retain the original FLH value for each sample point throughout the advection process; because diffusion and bloom ecology are not factored in, we do not model error in FLH estimates. Both will be addressed using Gaussian error processes that grow exponentially with time. Further we assume that the surface current field is constant within a neighborhood of the advected point. Our future work will address both these shortcomings.

Algorithm 1: Hotspot detection and advection

Input: MODIS images M_1 and M_2
Time period T = timestamp(M_2 - M_1)
t = t_{M_1}
$I_{\text{thresholded}}$ = threshold(M_1, F)
H = connectedSegments($I_{threholded}$)
h hotspots, H = $\{h_1, h_2, ..., h_k\}$
foreach *HotSpot* h_i **do**
    sample points for HotSpot h_i,
    P_i = resampleHotspot(h_i,resolution)
    P_i = $\{p_1, p_2, ..., p_N\}$
    foreach *sample point* p_j = $[x, y, t]$ **do**
        while $t < t_{m2}$ **do**
            $R_{p,t}$ = $[u, v]'$
            $p_{t+\Delta t} = p_t + R_{p,t}\Delta t$
            $\sigma_{p_{t+1}} = \sigma_{p_t} + \sigma_{R_t}\Delta t$
            $t = t + \Delta t$
        end
    end
end

TABLE I
HOTSPOT PROJECTION TEST CASES

Period(days)	Case	Evaluation Rating (max 5)
5	03/20/2008	3
4	06/02/2008	4
	10/12/2008	4
3	10/09/2008	4
2	10/12/2007	4.5
	02/15/2008	3
	03/18/2008	2
	03/25/2008	2
	04/10/2008	2
	04/26/2008	2
	05/21/2008	3
	10/10/2008	3.5
	10/12/2008	3
	10/14/2008	5
1	10/24/2007	4
	10/09/2008	2

III. ANALYSIS AND RESULTS

We performed advection of hotspots on a dataset of MODIS FLH images captured between September 2007 and November 2008 when both MODIS and HF Radar data were available. After rejecting unusable images (often due to cloud cover), we selected those that displayed hotspots of considerable intensity. We were also interested in studying the quality of advection for different time periods. From the test cases, we identified between 1 and 5 day periods between MODIS images to ground truth our projections. In total, we selected 16 test cases spanning the above period. The resulting projections, shown in Table I, were evaluated qualitatively by an oceanographer. We observed good predictions for stronger blooms, specifically those in the Fall. The advection of bloom patches fail to predict blooms that are in the initial stages of growth. However, the projections were good for blooms that were well developed and of high intensity. Fig. 7 and 8 show examples of two-day projection from the evaluated test cases.

IV. AN APPLICATION IN AUV SURVEYING

Our aim next is to choose an appropriate survey area given the prediction of a hotspot trajectory. A compelling scenario for such an application is illustrated in Fig. 9. Two day old satellite data shows the onset of a bloom. Our objective

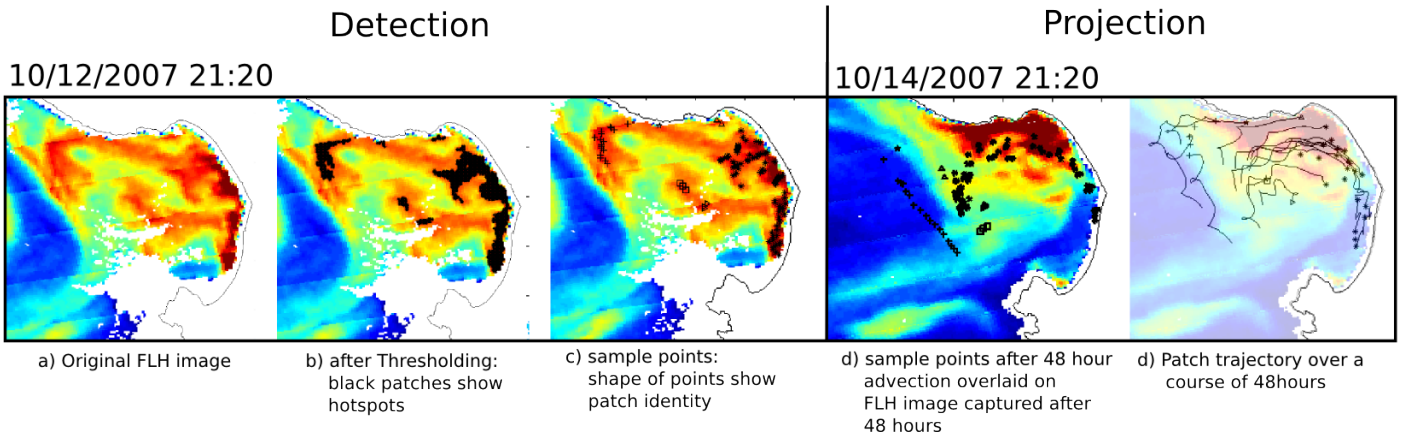

Fig. 7. Projection of a bloom from October 2007.

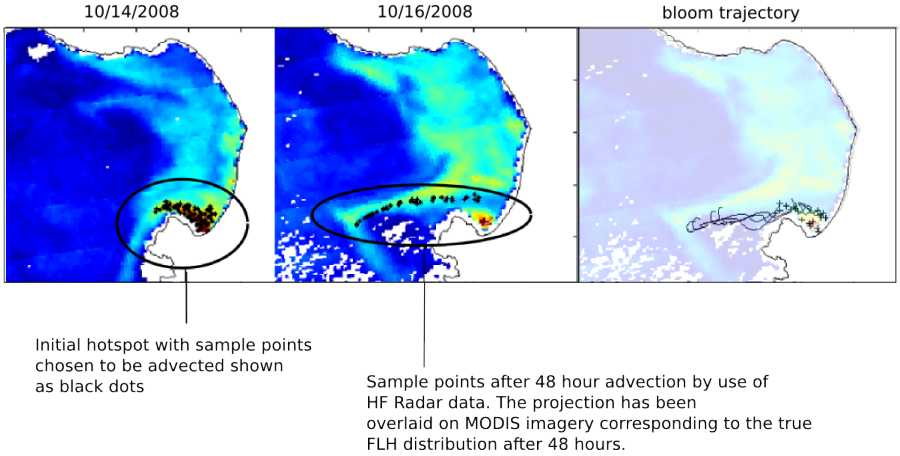

Fig. 8. Projection of a bloom from October 2008.

is to project the blooms trajectory and then place a viable 'lawnmower' AUV survey to ensure coverage.

A. Survey template

The 'lawnmower' pattern is a widely used survey pattern in oceanography primarily because of its uniform coverage and ease of subsequent data visualization as well as waypoint synthesis. We have designed our solution with the 'lawnmower' as the survey template, based on the constraints on the AUV *i.e.,* the runtime and the nominal velocity.

Let the maximum runtime be T and the nominal velocity of the AUV be v_{AUV}. The maximum distance that the AUV can cover is given by $L_{AUV} = Tv_{AUV}$. We define a pattern with the sides a and b, the swath width w and the length of the 'lawnmower' given by:

$$L = (\frac{a}{w} + 1)b + a \tag{1}$$

The bounding-box for the lawnmower is given by rectangle R, defined by the center p_c, sides a and b, and the angle θ the bounding box makes with the x-axis. We can nominally assume that the parameters of the bounding box that defines the survey area, are predecided. Using Equation 1, by choosing the sides of this bounding box, we can implicitly constrain the length of the 'lawnmower'. In later versions, we will relax this constraint. For a candidate survey area bounded by R, the sampling reward r is given by total signal intensity within the survey area. Since our goal is to attain maximum spatio-temporal sampling resolution at hotspots, our objective is to maximize the total signal intensity in the region where we sample. For our implementation, we define the sampling reward r as,

$$r = \sum_{i=0}^{n} e^{\alpha f_i} \cdot g_R(p_i) \tag{2}$$

where g is given by,

$$g(p) = \begin{cases} 1, & \text{if } p \text{ is inside rectangle R} \\ 0, & \text{if } p \text{ outside rectangle R} \end{cases} \tag{3}$$

and α is a chosen constant. The weighing function over FLH was chosen to be exponential to reward higher values of f favorably by a factor α. AUVs are nominally equipped with a suite of *in-situ* sensors that can sample additional parameters of interest in these regions where the expected chlorophyll concentration is high. For instance at MBARI, the upper water-column AUV is equipped with backscatter-based optical devices (Hobilabs HS2 and Sequoia Scientific Particle Size sensor), Satlantic/MBARI ISUS Nitrate sensor and a Seabird Dissolved Oxygen sensor in addition to two Seabird CTDs.

To determine the location and orientation for a survey with a known layout and dimension, we use a nested approach to search the survey area that maximizes the reward described by Equation 2. For our test case, we arbitrarily choose the length of the sides of the survey rectangle given by a and b

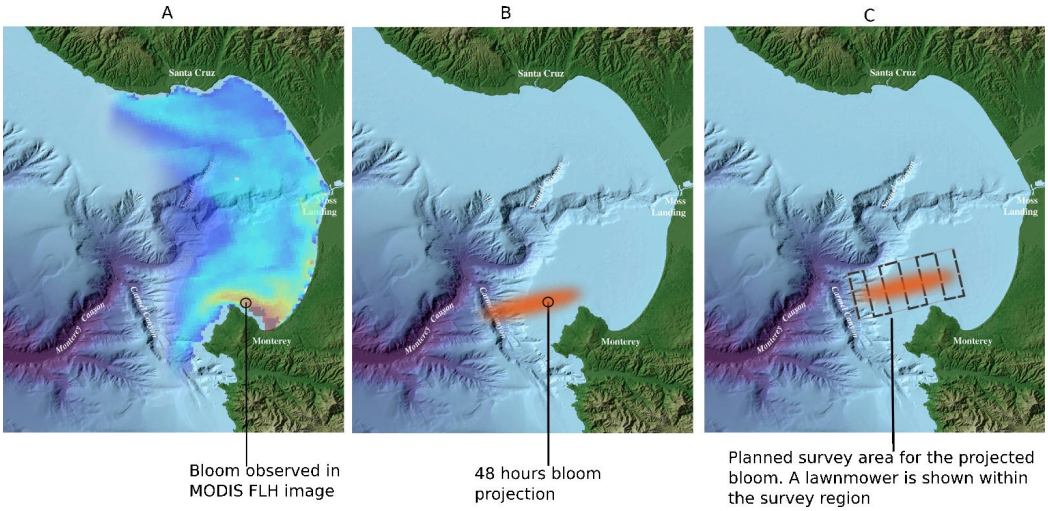

Fig. 9. A hypothetical bloom onset (A), projection (B) and a viable AUV survey to capture the bloom's spatial extent.

as 16km and 5km respectively. First, we find the bounding box of the projected sample points giving us the region of the ocean that has the maximum likelihood of an ongoing bloom based on our projection algorithm. Within this bounding box, we perform a recursive grid search. In each step, we split the bounding box into a 4x4 grid and compute the reward for each cell. We select the cell that has maximum reward, and continue the process. The recursion is terminated when the subsequent grid size is smaller than the survey area size. At this stage, we do an exhaustive search in the final cell (which would be larger than the survey-area since the grid search is terminated) to define the location and orientation of the survey-area. This is represented by $findBestArea$ in Algorithm 3.

Figs. 10 and 11 show the result of our search algorithm on the example bloom cases from October 2007 and 2008. The dotted box shows the initial bounding box and the solid box shows the final survey area chosen by the search algorithm.

Algorithm 2: recursiveBestGrid(G,a,b)

Input: survey area parameters a and b and grid G
L and B are length and breadth of bounding-box B
if $L/2 < a$ *OR* $B/2 < b$ **then**
    return G
end
$L = L/2, B = B/2$
$m = \arg\max_i(\text{samplingReward}(G_i, P))$
recursiveBestGrid(G_m,a,b)

Algorithm 3: findSurveyArea(P,a,b)

Input: N projected sample points $P = \{p_1, p_2, ..., p_N\}$
survey area parameters a and b
bounding-box of advected points B
G_{max} = recursiveBestGrid(B,a,b)
$[S_p, \theta]$ = findBestArea(G_{max},a,b)

The survey template places the AUV in the vicinity of the targeted hotspot. However once within the approximate area, the vehicle's adaptation and response to sensed pa-

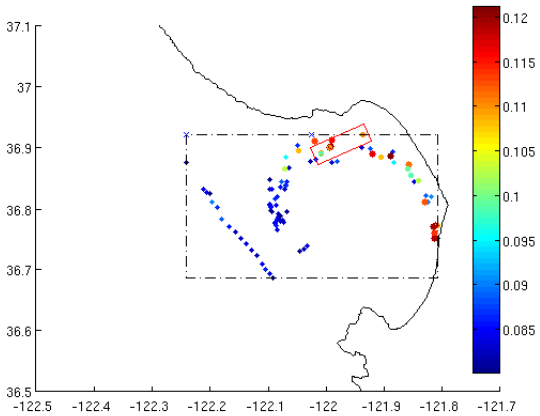

Fig. 10. Rectangular survey area of known size that maximizes the contained FLH intensity of the bloom case 1 (10/12/2007). The nested grid approach was used to search for the location and orientation of the rectangle that maximized the gain (FLH intensity).

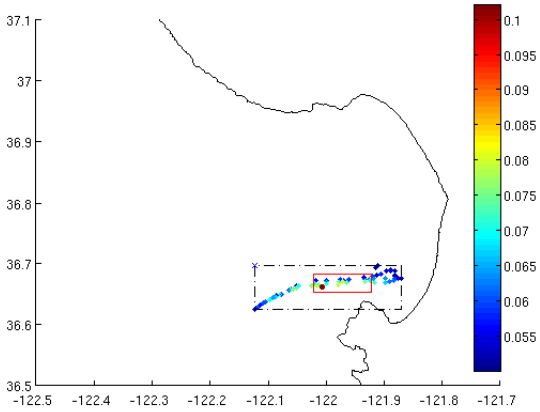

Fig. 11. Plot showing the survey rectangle for the October 2008 bloom

rameters needs to be considered. In this context we have been developing a framework for onboard autonomy, that integrates probabilistic state estimation, planning and execution. The Teleo-Reactive EXecutive (T-REX) is built upon the sense-plan-act [19] paradigm to autonomously synthesize control actions; re-planning to handle off nominal situations is automatic. Environmental state estimation uses a Hidden Markov Model (HMM) [20] to classify and enable online estimation based on offline machine learning techniques [21]. Additional details can be found in [22]–[25].

Together with the ability to track a patch of water, synthesize an abstract survey template and augmented by onboard autonomy, our toolchain can provide a viable way to track patches of water with specified properties. Our current focus on HABs provide a compelling science motivation with direct societal impact.

V. CONCLUSION AND FUTURE WORK

This paper presents an approach that can be used to generate survey missions for Autonomous Underwater Vehicles (AUVs) in the context of advected bloom patches. The approach uses remote sensing data to detect algal hotspots and projects these patches using surface current data from HF Radar stations along the central California coast. Result of advecting hotspots from blooms that occurred between October 2007 and October 2008 show that this approach is promising for tracking large, coherent blooms. Finally we show an example of how such predictions can be used to plan simple ('lawnmower' pattern) survey missions for AUVs. Our future work is to add more data sources such as in-situ platforms and vehicles as well as mooring and buoy data along with the incorporation of diffusion into the model to investigate various adaptive sampling methods and to motivate the HAB scenario to work towards multi-vehicle control.

VI. ACKNOWLEDGMENTS

This work was supported in part by the NOAA MERHAB program under grant NA05NOS4781228 and by NSF as part of the Center for Embedded Network Sensing (CENS) under grant CCR-0120778, by NSF grants CNS-0520305 and CNS-0540420, by the ONR MURI program (grants N00014-09-1-1031 and N00014-08-1-0693) by the ONR SoA program and a gift from the Okawa Foundation. We thank the David and Lucile Packard Foundation for supporting our work at MBARI.

REFERENCES

[1] E. Fiorelli, N. E. Leonard, S. Member, P. Bhatta, D. A. Paley, S. Member, R. Bachmayer, and D. M. Fratantoni, "Multi-auv control and adaptive sampling in monterey bay," in *IEEE Journal of Oceanic Engineering*, 2004, pp. 935–948.

[2] J. Binney, A. Krause, and G. S. Sukhatme, "Informative path planning for an autonomous underwater vehicle," in *IEEE International Conference on Robotics and Automation*, 2010.

[3] J. P. Ryan, H. M. Dierssen, R. M. Kudela, C. A. Scholin, K. S. Johnson, J. M. Sullivan, A. M. Fischer, E. V. Rienecker, P. R. McEnaney, , and F. P. Chavez, "Coastal ocean physics and red tides: an example from monterey bay, california," *Oceanography*, vol. 18, pp. 246–255, March 2005.

[4] D. Anderson, P. Hoagland, Y. Kaoru, and A. White, "Economic impacts from harmful algal blooms (HABs) in the United States," Woods Hole Oceanographic Institution Technical Report: WHOI 2000-11, Tech. Rep., 2000.

[5] P. Hoagland and S. Scatasta, *The Economic Effects of Harmful Algal Blooms*, E. Graneli and J. Turner, Eds. Springer-Verlag, 2006.

[6] Don Anderson, "Harmful algae," http://www.whoi.edu/redtide/page.do?pid=14898, 2008.

[7] J. P. Ryan, A. M. Fischer, R. M. Kudela, J. F. Gower, S. A. King, Marin, and F. P. Chavez, "Influences of upwelling and downwelling winds on red tide bloom dynamics in monterey bay, california," *Continental Shelf Research*, vol. 29, no. 5-6, pp. 785–795, March 2009. [Online]. Available: http://dx.doi.org/10.1016/j.csr.2008.11.006

[8] I. Cetinic, B. H. Jones, M. A. Moline, and O. Schofield, "Resolving urban plumes using autonomous gliders in the coastal ocean," *Journal of Geophysical Research/American Geophysical Union*, 2008.

[9] R. N. Smith, Y. Chao, B. H. Jones, D. A. Caron, P. P. Li, and G. S. Sukhatme, "Trajectory design for autonomous underwater vehicles based on oceanmodel predictions for feature tracking," in *Proceedings of the International Conference on Field and Service Robotics*, Jul. 2009.

[10] R. N. Smith, A. A. Pereira, Y. Chao, P. P. Li, D. A. Caron, B. H. Jones, and G. S. Sukhatme, "Autonomous underwater vehicle trajectory design coupled with predictive ocean models: A case study," in *IEEE International Conference on Robotics and Automation*, 2010.

[11] R. N. Smith, J. Das, H. Heiðarsson, A. A. Pereira, F. Arrichiello, I. Cetinić, L. Darjany, M. Ève Garneau, M. D. Howard, C. Oberg, M. Ragan, E. Seubert, E. C. Smith, B. Stauffer, A. Schnetzer, G. Toro-Farmer, D. A. Caron, B. H. Jones, and G. S. Sukhatme, "USC CINAPS Builds Bridges: Observing and Monitoring the Southern California Bight," *IEEE Robotics and Automation Magazine*, March 2010, special Issue on Marine Robotic Systems.

[12] A. F. Shchepetkin and J. C. McWilliams, "The regional oceanic modeling system (ROMS): A Split-explicit, Free-surface, Topography-following-coordinate Oceanic Model," *Ocean Modeling*, vol. 9, pp. 347–404, 2005.

[13] "The The Southern California Coastal Ocean Observing System (SCCOOS)." [Online]. Available: http://www.sccoos.org/

[14] "The Central and Northern California Ocean Observing System (CeNCOOS)." [Online]. Available: http://www.cencoos.org/

[15] "NASA Terra," http://terra.nasa.gov/.

[16] X.-G. Xing, D.-Z. Zhao, Y.-G. Liu, J.-H. Yang, P. Xiu, and L. Wang, "An overview of remote sensing of chlorophyll fluorescence," *Ocean Science Journal*, vol. 42, pp. 49–59, March 2007.

[17] R. M. Letelier and M. R. Abbott, "An analysis of chlorophyll fluorescence algorithms for the moderate resolution imaging spectrometer (modis)," *Remote Sensing of Environment*, vol. 58, pp. 215–223, 1996.

[18] "Red tide detection and tracing using modis fluorescence data: A regional example in sw florida coastal waters," *Remote Sensing of Environment*, vol. 97, no. 3, pp. 311 – 321, 2005.

[19] E. Gat, "On Three-Layer Architectures," in *Artificial Intelligence and Mobile Robots*, D. Kortenkamp, R. Bonnasso, and R. Murphy, Eds. MIT Press, 1998, pp. 195–210.

[20] L. R. Rabiner, "An introduction to hidden markov models," *IEEE ASSP Magazine*, pp. 4–16, 1986.

[21] M. Fox, D. Long, F. Py, K. Rajan, and J. P. Ryan, "In Situ Analysis for Intelligent Control," in *Proc. of IEEE/OES OCEANS Conference*. IEEE, 2007.

[22] C. McGann, F. Py, K. Rajan, H. Thomas, R. Henthorn, and R. McEwen, "A Deliberative Architecture for AUV Control," in *ICRA*, Pasadena, CA, May 2008.

[23] C. McGann, F. Py, K. Rajan, J. P. Ryan, and R. Henthorn, "Adaptive Control for Autonomous Underwater Vehicles," in *AAAI*, Chicago, IL, 2008.

[24] C. McGann, F. Py, K. Rajan, and A. Olaya, "Integrated Planning and Execution for Robotic Exploration," in *Intnl. Workshop on Hybrid Control of Autonomous Systems, in IJCAI09*, Pasadena, California, 2009.

[25] F. Py, K. Rajan, and C. McGann, "A Systematic Agent Framework for Situated Autonomous Systems," in *9th International Conf. on Autonomous Agents and Multiagent Systems*, Toronto, Canada, May 2010.